



Cadmium(II) and indium(III) complexes derived from 2-benzoylpyridine *N*(4)-cyclohexylthiosemicarbazone: Synthesis, crystal structures, spectroscopic characterization and cytotoxicity

Yan-Xue Tai, Yu-Mei Ji, Yan-Li Lu, Ming-Xue Li*, Yuan-Yuan Wu, Qiu-Xia Han*

Key Laboratory of Polyoxometalates of Henan Province, Institute of Molecular and Crystal Engineering, College of Chemistry and Chemical Engineering, Henan University, Kaifeng 475004, PR China

ARTICLE INFO

Article history:

Received 21 March 2016
Received in revised form 6 May 2016
Accepted 14 May 2016
Available online xxx

Keywords:

Thiosemicarbazone
Crystal structure
Cytotoxicity
Fluorescent probe

ABSTRACT

Two metal complexes $[\text{Cd}(\text{L})_2] \cdot 0.275\text{H}_2\text{O}$ (**1**) and $[\text{In}(\text{L})_2]\text{NO}_3$ (**2**) (HL = 2-benzoylpyridine *N*(4)-cyclohexylthiosemicarbazone) have been synthesized and structurally characterized by elemental analysis, a number of spectroscopic methods (IR, UV-vis, NMR), mass spectrometry, and X-ray crystallography. The Schiff's base ligand forms hexacoordinated complexes having octahedral geometry for Cd(II) and In(III) complexes, respectively. The synthesized compounds were tested for antiproliferative activity and showed the ability to kill HepG2 cells (human hepato cellular carcinoma) significantly, especially **2** with $\text{IC}_{50} = 2.02 \pm 0.14 \mu\text{M}$. Of particular note is the fact that complex **1** has *ca* 12-fold lower toxicity in the normal hepatocyte QSG7701 cells than in the hepatocellular carcinoma HepG2 cells. In addition, complex **2** also exhibited excellent luminescent property. Upon the addition of 1 equiv of In^{3+} ion, 200-fold fluorescence enhancement of HL at $\lambda_{\text{em}} = 504 \text{ nm}$ has been observed. Moreover, the fluorescent color change (from transparent to light-green) could be observed by naked eyes under the light of 365 nm. These findings can expand the applications of thiosemicarbazone derivatives in the fields of colorimetric and fluorescent probes.

© 2016 Elsevier B.V. All rights reserved.

1. Introduction

From the early 1950s to the present, the chemistry of thiosemicarbazones has shown considerable interest in analytical chemistry, pharmacological properties and spectrophotometry [1–5]. The best known member of this family, 3-aminopyridine carboxaldehyde thiosemicarbazone (3-AP), is a potent ribonucleotide reductase inhibitor that is currently in phase II clinical trials for the treatment of a number of forms of cancer, including non-small-cell lung cancer and renal carcinoma [6]. This compound shows therapeutic activity over a certain range of dosages in preclinical tumor models without imposing intolerable host toxicity [7]. In more cases, the involvement of mixed nature of the N and S donor atoms in coordination with metal ions is responsible for increasing biological activities of thiosemicarbazones [8,9]. Their mechanism of action is still controversial in many respects, including ribonucleotide reductase inhibition, metal

dependent radical damage, DNA binding, and inhibition of protein synthesis [10,11].

Cadmium is an extremely toxic element whose deleterious actions influence the majority of human tissues and is often present in the environment [12]. Its toxicity derives from the fact that it is rapidly localized intracellularly, mainly in the liver, and then is bound to metallothionein forming a complex that is slowly transferred to the bloodstream to be deposited in the kidneys. Even so, cadmium complexes have attracted more and more attentions due to their widely reported bioactivities, such as DNA binding ability [13], antibacterial activities [14] and antitumor activities [15,16]. Moreover, the compounds which are able to form stable complexes with cadmium could be employed as detoxifying agents [14].

Indium is an auger electron emitter, potentially enabling its complexes to be dual imaging-therapeutic agents [17]. However, indium complexes remain relatively unexplored to date [18–21]. Therefore, detailed investigations of indium complexes will be valuable.

As part of our systematic studies on heterocyclic thiosemicarbazones and their metal complexes [8,22–25], here we report the synthesis, characterization and *in vitro* cytotoxicity of Cd(II)

* Corresponding authors.

E-mail addresses: limingxue@henu.edu.cn (M.-X. Li), hdhqx@henu.edu.cn (Q.-X. Han).

and In(III) complexes formulated as $[\text{Cd}(\text{L})_2] \cdot 0.275\text{H}_2\text{O}$ (**1**), $[\text{In}(\text{L})_2] \text{NO}_3$ (**2**) (HL = 2-benzoylpyridine *N*(4)-cyclohexylthiosemicarbazone) (Scheme 1). In addition, luminescent studies have been carried out.

2. Experiment

2.1. Materials and methods

All solvents and reagents used in this study were reagent grade and used without further purification. The melting points were determined with a Gallenkamp electrically heated apparatus. Elemental analyses (C, H and N) were performed on a Perkin-Elmer 2400-II analyzer. Inductively coupled plasma (ICP) analysis was performed on a Jarrel-AshJ-A1100 spectrometer. The IR spectrum was recorded on a Nicolet FT-IR 360 spectrometer using KBr pellets in the range of $4000\text{--}400\text{ cm}^{-1}$. The UV-vis absorption spectrum was obtained with a U-4100 spectrometer at room temperature. The mass spectra (MS) were taken out on an Esquire 3000 LC-MS mass spectrometer. ^1H NMR spectra were recorded in $\text{DMSO-}d_6$ using a Bruker AV-400 spectrometer. The fluorescent emission spectrums were collected on a HITACHI F-7000 model instrument.

2.2. Synthesis

2.2.1. Synthesis of ligand (HL)

The ligand HL was synthesized according to the literature [26] and confirmed by the IR spectrum.

2.2.2. Synthesis of complex 1

A methanol solution containing $\text{Cd}(\text{ClO}_4)_2 \cdot 6\text{H}_2\text{O}$ (0.084 g, 0.2 mmol) was added dropwise to a methanol solution (20 mL) of 2-benzoylpyridine *N*(4)-cyclohexylthiosemicarbazone (0.136 g, 0.4 mmol) and NaOAc (0.032 g, 0.4 mmol). After refluxing for 1 h with stirring, the resultant mixture was filtered. The obtained solid product was subsequently purified by recrystallization from methanol and dried over P_4O_{10} *in vacuo*. Yield: 70%, M.P.

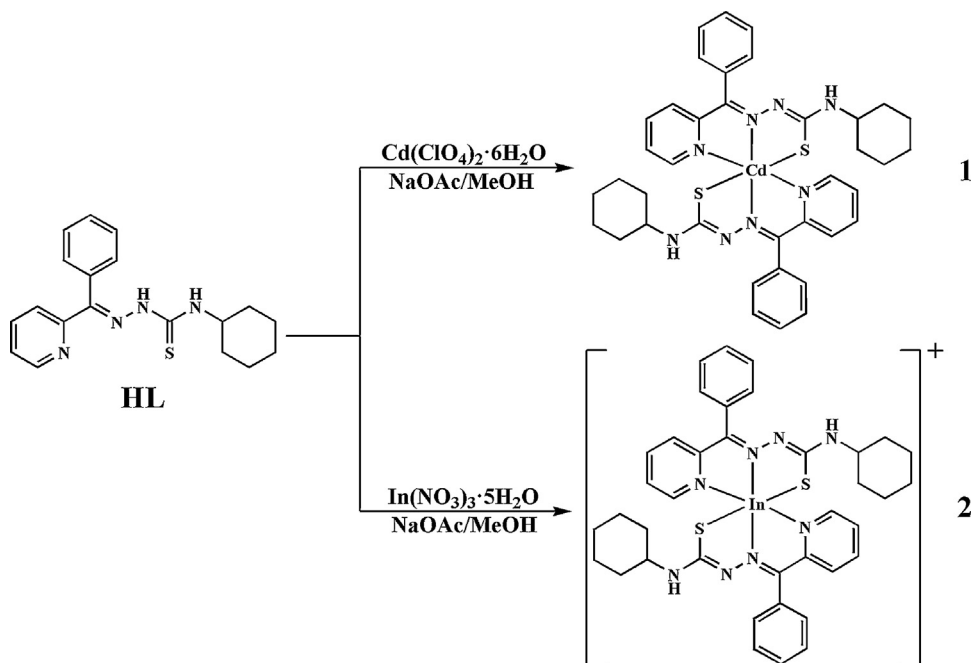
$245\text{--}246\text{ }^\circ\text{C}$, Elemental analysis calcd for $\text{C}_{38}\text{H}_{42.55}\text{CdN}_8\text{O}_{0.275}\text{S}_2$ (**1**): C, 57.61; H, 5.41; N, 14.14; Cd, 14.19. Found: C, 57.85; H, 5.46; N, 14.05; Cd, 14.26. ESI-MS (m/z): $789.2 = [\text{Cd}(\text{L})(\text{HL})]^+$ (Fig. S1 in the Supporting information). calc: mass = 789.2. ^1H NMR ($\text{DMSO-}d_6$, δ ppm) 8.48 (s, 1H, NH), 8.09 (s, 1H, Py), 7.79 (s, 1H, Py), 7.52–7.46 (m, 3H, Ph), 7.38 (d, $J = 4\text{ Hz}$, 2H, Ph), 7.25–7.22 (m, 1H, Py), 7.07 (d, $J = 5.6\text{ Hz}$, 1H, Py), 1.75 (s, 11H, C_6H_{11}). Yellow crystals suitable for X-ray studies were obtained by the slow evaporation of a methanol solution of **1**.

2.2.3. Synthesis of complex 2

Complex **2** was prepared by a similar procedure to that of complex **1** using $\text{In}(\text{NO}_3)_3 \cdot 5\text{H}_2\text{O}$ (0.078 g, 0.2 mmol) in place of Cd (ClO_4) $_2 \cdot 6\text{H}_2\text{O}$ (0.084 g, 0.2 mmol). Yield: 85%, M.P. $224\text{--}227\text{ }^\circ\text{C}$, Elemental analysis calcd for $\text{C}_{38}\text{H}_{42}\text{InN}_9\text{O}_3\text{S}_2$ (**2**): C, 53.58; H, 4.97; N, 14.80; In, 13.48. Found: C, 53.38; H, 4.72; N, 14.85; In, 13.58. ESI-MS (m/z): $789.2 = [\text{In}(\text{L})_2]^+$ (Fig. S2 in the Supporting information). calc: 789.2. ^1H NMR ($\text{DMSO-}d_6$, δ ppm) 8.12 (s, 1H, NH), 7.75 (t, $J = 6.4\text{ Hz}$, 2H, Py), 7.62–7.54 (m, 4H, Ph), 7.46 (d, $J = 8\text{ Hz}$, 1H, Py), 7.32 (t, $J = 8.8\text{ Hz}$, 1H, Ph), 7.21 (d, $J = 8\text{ Hz}$, 1H, Py), 1.81–1.00 (m, 11H, C_6H_{11}). Yellow crystals suitable for X-ray studies were obtained by the slow evaporation of a methanol solution of **2**.

2.3. X-ray crystallography

Crystallographic data were collected with a Bruker SMART-CCD APEX II diffractometer with graphite-monochromated Mo $K\alpha$ radiation ($\lambda = 0.71073\text{ \AA}$). The structures were solved by direct methods and refined by full-matrix least squares on F^2 with anisotropic displacement parameters for all non-hydrogen atoms using SHELXTL [27]. Although the higher R_{int} value of 0.1251 (>0.10) for **1** is somewhat large, owing to poor crystal quality, the molecule skeleton is well behaved, and there are no unusual temperature factors in the structure. The atoms of O1, O2, O3 and N9 of the nitrate anion from **2** were refined isotropically to avoid the ADP errors. The hydrogen atoms were added in idealized geometrical positions. Crystal data, experimental details, and refinement results are listed in Table 1.



Scheme 1. 2-benzoylpyridine *N*(4)-cyclohexylthiosemicarbazone (HL) and the reaction scheme for the synthesis of **1** and **2**.

Table 1
Crystallographic data and structural refinements for **1** and **2**.

	1	2
Empirical formula	C ₃₈ H _{42.55} CdN ₈ O _{0.275} S ₂	C ₃₈ H ₄₂ InN ₉ O ₃ S ₂
Formula weight (g·mol ⁻¹)	792.29	851.74
T (K)	293(2)	296(2)
Crystal system	Monoclinic	Monoclinic
space group	C2/c	Cc
a (Å)	30.057(18)	17.9751(14)
b (Å)	14.596(9)	13.6158(11)
c (Å)	18.951(11)	16.8775(13)
α (deg)	90.00	90.00
β (deg)	109.860(11)	107.673(2)
γ (deg)	90.00	90.00
V (Å ³)	7820(8)	3935.7(5)
Z	8	4
D _c (g·cm ⁻³)	1.338	1.437
μ (mm ⁻¹)	0.702	0.755
Limiting indices	-35 ≤ h ≤ 35 -17 ≤ k ≤ 17 -22 ≤ l ≤ 20	-21 ≤ h ≤ 8 -16 ≤ k ≤ 16 -20 ≤ l ≤ 20
R _{int}	0.1251	0.0283
Restraints/parameters	37/443	333/455
θ range (°)	2.081–25.099	1.911–25.095
Goodness-of-fit on F ²	0.872	1.029
R ₁ , wR ₂ [I > 2σ(I)]	0.0663, 0.1599	0.0724, 0.1948
R ₁ , wR ₂ [all data]	0.1371, 0.1823	0.0985, 0.2227

2.4. Fluorescence measurements

For fluorescence behavior, stock methanol solutions (10⁻³ mol·L⁻¹) of HL, In(NO₃)·5H₂O, **1** and **2** were prepared. The solution of HL, **1** and **2** were then diluted to 10⁻⁴ mol·L⁻¹ with methanol. In concentration gradients experiments, HL (1 mL, 10⁻³ mol·L⁻¹) and appropriate amounts of In³⁺ (0, 125, 250, 500, 750, 1000 μL) were added to a volumetric flask (10 mL), and then added methanol to 10 mL, respectively. For fluorescence measurements, excitation was provided at 361 nm, and emission was acquired from 371 nm to 730 nm.

2.5. Cell culture

The hepatocellular carcinoma HepG2 cells and the normal hepatocyte QSG7701 cells were cultured in Dulbecco's minimal essential medium supplemented with 10% fetal bovine serum, 100 IU·mL⁻¹ penicillin, and 100 μg·mL⁻¹ streptomycin at 37 °C in a humidified atmosphere with 5% CO₂. The cells were harvested with 0.02% EDTA and 0.025% trypsin and then rinsed three times in phosphate-buffered saline (PBS). The resulting cell suspension was used in following experiment.

2.6. Cytotoxicity assay

3-(4,5-Dimethylthiazol-2-yl)-2,5-diphenyltetrazolium bromide (MTT) assay was carried out to evaluate cytotoxicity. Cells were plated into 96-well plates at a cell density of 1 × 10⁴ cells per well and allowed to grow in a CO₂ incubator. After 24 h, the medium was removed and replaced by fresh medium containing the tested compounds which were dissolved in DMSO at 0.01 M and diluted to various concentrations with PBS before the experiment, and the final concentration of DMSO is lower than 1%. After 24 h incubation, cultures were incubated in 100 μL of medium with 10 μL of 5 mg/mL MTT solution for 4 h at 37 °C. The medium with MTT was removed, and 100 μL of dimethyl sulfoxide (DMSO) was added to each well to dissolve the formazan. The absorbance at 570 nm was measured with microplate reader (Bio-Tek ELX800, USA). The inhibitory percentage of each compound at various concentrations was calculated, and the IC₅₀ value was

determined. All data are expressed as the mean ± SD from three separate determinations.

3. Results and discussion

3.1. X-ray crystallography

Selected bond distances and angles of **1** and **2** are given in Table 2. The molecular structures along with the atom numbering scheme and the unit cell packing are depicted in Figs. 1 and 2, respectively.

3.1.1. Crystal structure of **1**

As shown in Fig. 1a, the two N,N,S-coordinated ligands give the Cd(II) ion a highly distorted octahedral coordination polyhedron. One sulfur atom, one imine nitrogen atom and one pyridine nitrogen atom from one ligand and one imine nitrogen atom from another ligand occupy the basal positions, the two remaining positions in the octahedral geometry are the axial ones which are occupied by one sulfur atom and one pyridine nitrogen atom from the second ligand. The pseudo-macrocyclic coordination mode of each ligand affords two five-membered chelate rings, the dihedral angle between the chelate rings are 12.6 and 12.8°, respectively. Both C–S bond lengths suggest evolution towards the thiol form. The C–N and N–N bond lengths in L⁻ are intermediate between formal single and double bonds, pointing to an extensive electron delocalization over the entire molecular skeleton [28]. Similarly, intermolecular hydrogen bonds of complex **1** also link the different components to stabilize the crystal structure (Fig. 1b and c). The hydrogen bond involves the terminal nitrogen atom N(5) and the coordinated sulfur atom S(2) with N(5)···S(2) 3.422(7) Å and the angle N(5)–H(5A)···S(2) being 161.9° (symmetry code: -x + 1/2, -y + 1/2, -z), respectively.

3.1.2. Crystal structure of **2**

As shown in Fig. 2a, the molecular structure of **2** contains one [In(L)₂]⁺ cation and one nitrate ion acting as the counterion. The indium(III) ion has the same coordination model as cadmium(II) in complex **1**. The pseudo-macrocyclic coordination mode of each ligand affords two five-membered chelate rings, which are near planar, the dihedral angle between the chelate rings are 3.4 and

Table 2
Selected bond lengths (Å) and bond angles (°) of complexes **1** and **2**.

1		2	
Cd(1)–S(1)	2.564(3)	In(1)–S(1)	2.506(4)
Cd(1)–S(2)	2.565(2)	In(1)–S(2)	2.493(5)
Cd(1)–N(3)	2.410(6)	In(1)–N(3)	2.262(13)
Cd(1)–N(4)	2.406(7)	In(1)–N(4)	2.323(14)
Cd(1)–N(7)	2.389(6)	In(1)–N(7)	2.268(13)
Cd(1)–N(8)	2.390(6)	In(1)–N(8)	2.326(13)
S(1)–C(7)	1.735(8)	S(1)–C(7)	1.743(16)
S(2)–C(26)	1.730(7)	S(2)–C(26)	1.756(18)
N(3)–C(8)	1.328(9)	N(3)–C(8)	1.29(2)
N(7)–C(27)	1.287(8)	N(7)–C(27)	1.33(2)
N(8)–Cd(1)–N(4)	92.3(2)	N(7)–In(1)–N(8)	71.5(4)
N(4)–Cd(1)–N(3)	67.6(2)	N(3)–In(1)–N(4)	70.5(5)
N(3)–Cd(1)–S(1)	73.40(18)	N(7)–In(1)–N(4)	90.4(5)
N(4)–Cd(1)–S(1)	137.31(17)	N(4)–In(1)–N(8)	91.8(5)
N(7)–Cd(1)–S(2)	73.59(15)	N(4)–In(1)–S(2)	93.5(4)
N(8)–Cd(1)–S(2)	137.50(15)	N(3)–In(1)–S(1)	77.9(3)
S(1)–Cd(1)–S(2)	97.10(8)	N(7)–In(1)–S(1)	121.4(4)
C(7)–S(1)–Cd(1)	99.0(3)	N(8)–In(1)–S(1)	93.4(4)
C(26)–S(2)–Cd(1)	98.5(3)	N(4)–In(1)–S(1)	147.7(4)
C(27)–N(7)–Cd(1)	121.1(5)	C(7)–S(1)–In(1)	94.9(6)
N(6)–N(7)–Cd(1)	121.4(5)	C(26)–S(2)–In(1)	96.2(6)
		C(8)–N(3)–In(1)	120.0(11)
		N(2)–N(3)–In(1)	122.4(10)

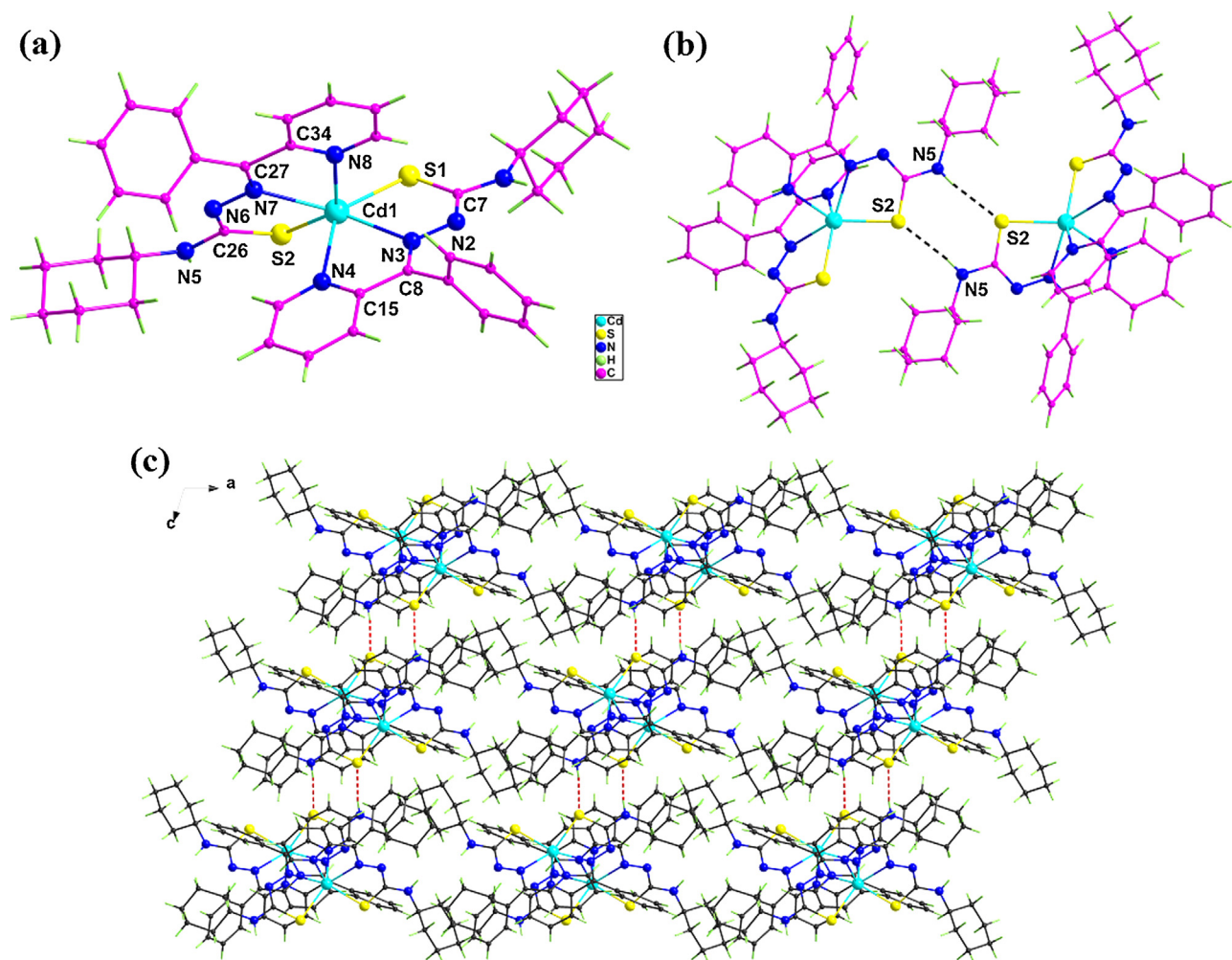


Fig. 1. (a) Structure of complex 1 with atomic numbering scheme. (b) Hydrogen bond indicated by dashed line. (c) The molecular packing projected along the b-axis.

5.1°, respectively. Fig. 2b is the molecular packing projected along the b-axis.

3.2. Infrared spectra

The characteristic vibrational bands of HL, **1** and **2** corresponding to the important functions in the system are presented in Table 3. The free ligand shows two bands at 3336 and 3162 cm^{-1}

observed at 3285 and 3236 cm^{-1} in complexes **1** and **2** instead, respectively. These bands may be assigned for N–H stretching vibrations. The $\nu(\text{C}=\text{N})$ bands of thiosemicarbazone in two complexes undergoes a red shift of wavenumber compared to that of the ligand (1523 cm^{-1}), a clear sign of coordination via the imine nitrogen atom. Additionally, the increase in the frequency of $\nu(\text{N}-\text{N})$ band of the thiosemicarbazone in the spectra of complexes is due to the increase in the bond strength, again confirms the

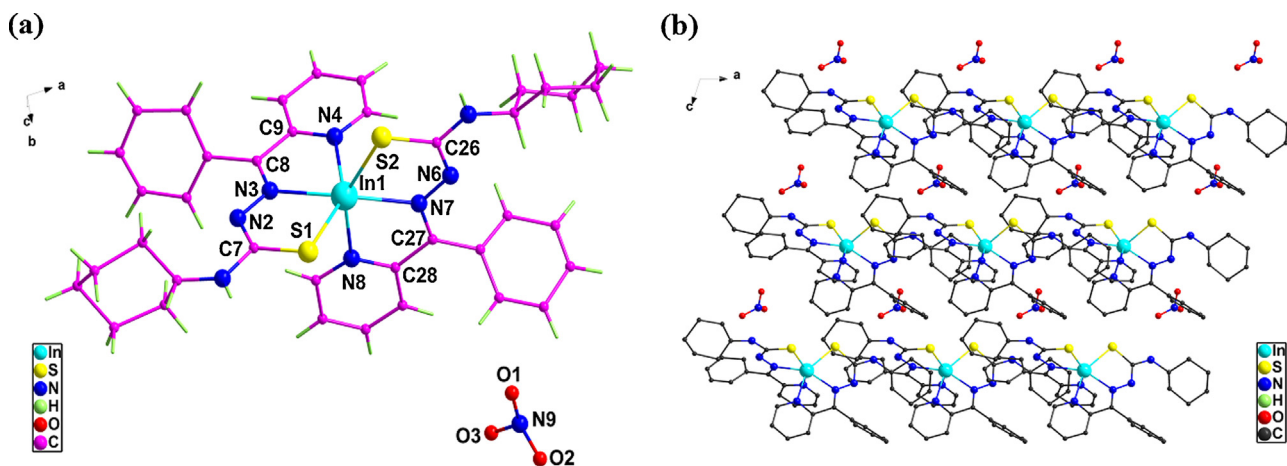


Fig. 2. (a) Structure of complex 2 with atomic numbering scheme. (b) The molecular packing projected along the b-axis.

Table 3
Infrared spectral assignments for the ligand HL, **1** and **2**.

Compound	$\nu(\text{N-H})$	$\nu(\text{C=N})$	$\nu(\text{N-N})$	$\nu(\text{C=S})$	$\nu(\text{py})$
HL	3336, 3162	1523	1119	800	608
1	3285	1494	1147	787	627
2	3236	1496	1152	781	643

coordination *via* the imine nitrogen [4]. The thioamide band, which contains considerable $\nu(\text{C=S})$ character, is less intense in the complexes and is found at a lower frequency, suggesting coordination of the metal through sulfur [29]. The pyridyl nitrogen resulting breathing motion of the pyridine ring is shifted to a higher frequency upon complexation and is consistent with pyridine ring nitrogen coordination. These observations have indicated the participation of imine nitrogen, thiolate sulfur and pyridine nitrogen of the ligand in the coordination.

3.3. UV-vis spectra

The UV-vis spectra of these compounds were studied in methanol solution. As shown in Fig. 3 the ligand HL gives two band at 322 and 410 nm, while complex **1** exhibits two peaks of 302 and 398 nm in ultraviolet region and complex **2** exhibits one band of 302 nm in ultraviolet region and one peak of 408 nm in visible region. These compounds have a band in the range 302–322 nm due to $\pi \rightarrow \pi^*$ transitions, while the strong absorption at 398 (**1**) and 408 (**2**) nm may be attributed to the LMCT transitions. Such a feature provides a good evidence for the chelation of the ligand to the metal centre.

3.4. Fluorescence spectral studies

The fluorescence behaviors of these compounds (HL, **1** and **2**) were studied in 1×10^{-4} M methanol solution. Fluorescence experiments were carried out with 361, 354 and 333 nm as excitation wavelength of HL, **1** and **2**, respectively. The spectral changes of HL, **1** and **2** are shown in Fig. 4. It can be seen that the three compounds show different emission peaks at 406, 400 and 537, 371 and 508 nm, respectively and the complex **2** exhibits a strong fluorescence emission at 508 nm. The results indicated that different metal complexes had a significant effect not only on the emission peak but also on the emission intensity [30]. The titration experiments were carried out by adding different concentrations of indium(III) ion. Upon the addition of 1 equiv of In^{3+} ion, 200-fold fluorescence enhancement of HL has been observed. Furthermore,

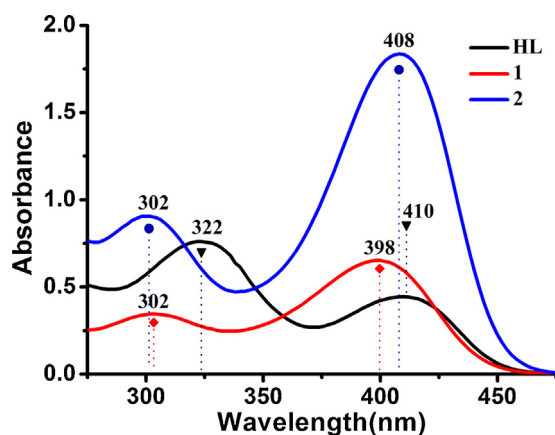


Fig. 3. UV-vis absorption spectra of the HL, **1** and **2** in methanol solution at room temperature.

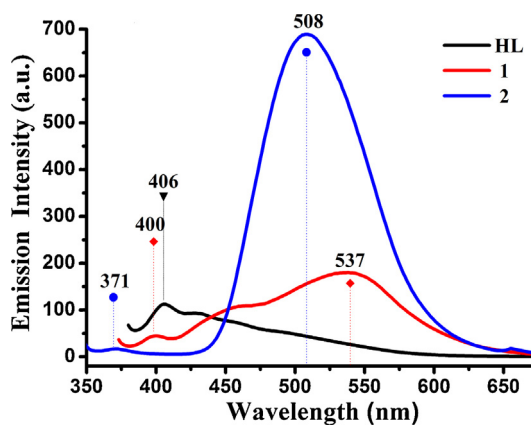


Fig. 4. Fluorescence emission spectra of HL, **1** and **2** in methanol solution at room temperature.

the visual fluorescence response can be seen under UV light (Fig. 5b). This phenomenon indicates that this ligand can be used as a sensitive probe for In^{3+} .

3.5. Cytotoxicity assay

In terms of the cytotoxic activity of thiosemicarbazones [31], firstly, we have evaluated the ability of HL and complexes **1** and **2** to inhibit tumor cell growth against HepG2 cells. To explore the toxicity of these compounds, their effect on normal QSG7701 cells is also described. In our experiments, IC_{50} values (compound concentration that produces 50% of cell death) in micromolar units are calculated (Fig. 6). Mitoxantrone (Mito) is a synthetic antineoplastic drug and widely used as a potent chemotherapeutic agent in the treatment of various types of cancer because of its apparent lower risk of cardio-toxic effects. Therefore, mitoxantrone was employed as the reference compound for comparison.

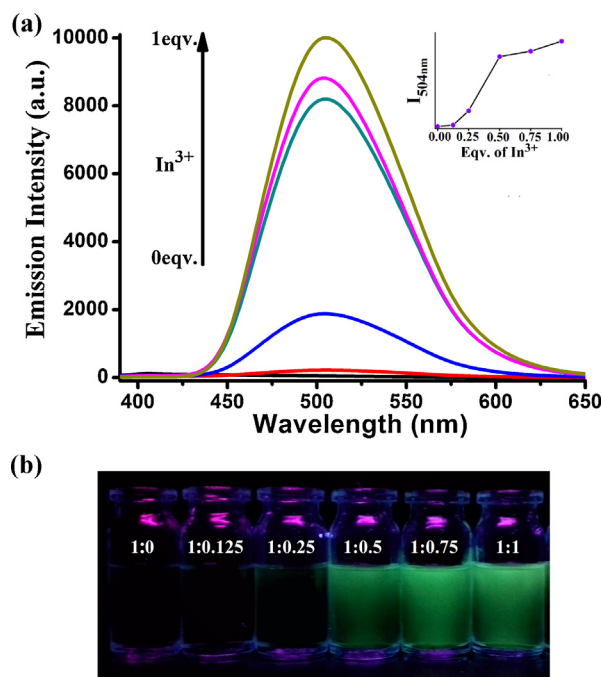


Fig. 5. (a) Fluorescence emission spectra of HL in the absence and presence of In^{3+} (methanol solvent) at 504 nm, $\lambda_{\text{exc}} = 361$ nm, voltage 700 V, Concentration of HL 10^{-4} M. INSET Changes in the emission intensity at 504 nm with incremental addition of In^{3+} (b) Visual changes observed for HL in the presence of different equivalents In^{3+} under UV lamp (365 nm).

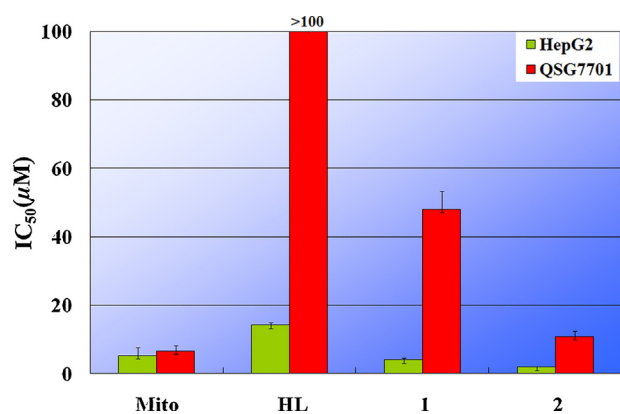


Fig. 6. The cytotoxicity of the tested compounds against HepG2 cells and QSG7701 cells. All data are expressed as the mean \pm SD from three separate determinations.

As shown in Fig. 6, the title compound indicated significant cytotoxicity and complexes **1** and **2** show much lower IC_{50} values ($4.02 \pm 0.57 \mu\text{M}$, $2.02 \pm 0.14 \mu\text{M}$, respectively) than HL ($14.26 \pm 0.68 \mu\text{M}$) against HepG2 cells. It should be emphasized that complex **2** effectively inhibit HepG2 cells at concentrations 7-fold lower than the free ligand. Importantly, IC_{50} values of all the tested compounds are obviously higher in QSG7701 cells ($>100 \mu\text{M}$, $48.04 \pm 5.25 \mu\text{M}$, $10.86 \pm 1.61 \mu\text{M}$ for HL, **1** and **2**, respectively) than in HepG2 cells indicating they are lower toxicity against QSG7701 cells. Of particular note is the fact that complex **1** has *ca* 12-fold lower toxicity in the normal hepatocyte QSG7701 cells than in the hepatocellular carcinoma HepG2 cells. Therefore, the compounds studied in the present work would be good candidates to be used for medical practice as metal-based drugs.

4. Conclusions

Two metal complexes $[\text{Cd}(\text{L})_2] \cdot 0.275\text{H}_2\text{O}$ (**1**) and $[\text{In}(\text{L})_2]\text{NO}_3$ (**2**) (HL = 2-benzoylpyridine-*N*(4)-cyclohexylthiosemicarbazone) have been synthesized and structurally characterized. The synthesized compounds showed the ability to kill liver cancer cells significantly and could distinguish the human hepatocellular carcinoma HepG2 cells from normal hepatocyte QSG7701 cells. The detection of 2-benzoylpyridine-*N*(4)-cyclohexylthiosemicarbazone for In^{3+} is studied by fluorescence spectra. This ligand can be used as a sensitive probe for In^{3+} . These findings can expand the applications of thiosemicarbazone derivatives in the fields of colorimetric and fluorescent probes.

Supplementary data

CCDC reference numbers 920504 and 920505 contain the supplementary crystallographic data for **1** and **2**, respectively. These data can be obtained free of charge from the Cambridge Crystallographic Centre via www.ccdc.cam.ac.uk/data_request/cif.

Acknowledgements

This work was financially supported by the National Natural Science Foundation of China (21071043, U1304201), and the

Natural Science Foundation of the Educational Department of Henan Province (14B150028).

Appendix A. Supplementary data

Supplementary data associated with this article can be found, in the online version, at <http://dx.doi.org/10.1016/j.synthmet.2016.05.015>.

References

- [1] M. Jagadeesh, S.K. Kalangi, L.S. Krishna, A.V. Reddy, Spectrochim. Acta Part A 118 (2014) 552–556.
- [2] M. Jagadeesh, H.K. Rashmi, Y.S. Rao, A.S. Reddy, B. Prathima, P.U.M. Devi, A.V. Reddy, Spectrochim. Acta Part A 115 (2013) 583–587.
- [3] M. Tyagi, S. Chandra, P. Tyagi, Spectrochim. Acta Part A 117 (2014) 1–8.
- [4] S. Chandra, S. Bargujar, R. Nirwal, K. Qanungo, S.K. Sharma, Spectrochim. Acta Part A 113 (2013) 164–170.
- [5] M. Shebl, M.A. Ibrahim, S.M.E. Khalil, S.L. Stefan, H. Habib, Spectrochim. Acta Part A 115 (2013) 399–408.
- [6] C.R. Kowol, R. Trondl, P. Heffeter, V.B. Arion, M.A. Jakupec, A. Roller, M. Galanski, W. Berger, B.K. Keppler, J. Med. Chem. 52 (2009) 5032–5043.
- [7] R.A. Finch, M.C. Liu, S.P. Grill, W.C. Rose, R. Loomis, K.M. Vasquez, Y.C. Cheng, A. C. Sartorelli, Biochem. Pharmacol. 59 (2000) 983–991.
- [8] N. Zhang, Y.X. Tai, M.X. Li, P.T. Ma, J.W. Zhao, J.Y. Niu, Dalton Trans. 43 (2014) 5182–5189.
- [9] B. Shaabani, A. Khandar, M. Dusek, M. Pojarova, F. Mahmoudi, Inorg. Chim. Acta 394 (2013) 563–568.
- [10] K.A. Price, A. Caragounis, B.M. Paterson, G. Filiz, I. Volitakis, C.L. Masters, K.J. Barnham, P.S. Donnelly, P.J. Crouch, A.R. White, J. Med. Chem. 52 (2009) 6606–6620.
- [11] B. Garcia, J. Garcia-Tojal, R. Ruiz, R. Gil-Garcia, S. Ibeas, B. Donnadieu, J.M. Leal, J. Inorg. Biochem. 102 (2008) 1892–1900.
- [12] K.N. Tzirogiannis, G.I. Panoutsopoulos, M.D. Demonakou, G.K. Papadimas, V.G. Kondyli, K.T. Kourantzi, R.I. Hereti, M.G. Mykoniatis, Arch. Toxicol. 78 (2004) 321–329.
- [13] F. Zhang, X.L. Zheng, Q.Y. Lin, P.P. Wang, W.J. Song, Inorg. Chim. Acta. 394 (2013) 85–91.
- [14] K. Alomar, A. Landreau, M. Kempf, M.A. Khan, M. Allain, G. Bouet, J. Inorg. Biochem. 104 (2010) 397–404.
- [15] S. Bjelogrić, T. Todorovc, A. Bacchi, M. Zec, D. Sladic, T. Srdic-Rajic, D. Radanovic, S. Radulovic, G. Pelizzi, K. Anđelkovic, J. Inorg. Biochem. 104 (2010) 673–682.
- [16] X.P. Zhou, Y. Koizumi, M. Zhang, M. Natsui, S. Koyota, M. Yamada, Y. Kondo, F. Hamada, T. Sugiyama, Cancer Sci. 106 (2015) 635–641.
- [17] J. Chan, A.L. Thompson, M.W. Jones, J.M. Peach, Inorg. Chim. Acta 363 (2010) 1140–1149.
- [18] S. Abram, C. Maichle-Mossmar, U. Abram, Polyhedron 17 (1998) 131–143.
- [19] Y.J. Fan, L. Wang, J.P. Ma, Acta Crystallogr. Sect. E: Struct. Rep. Online E63 (2007) m261–m262.
- [20] Y.J. Fan, L. Wang, J.P. Ma, Z.X. Sun, Acta Crystallogr. Sect. E: Struct. Rep. Online E63 (2007) m845–m846.
- [21] C. Paek, S.O. Kang, J. Ko, P.J. Carroll, Organometallics 16 (1997) 4755–4758.
- [22] Y.K. Li, M. Yang, M.X. Li, H. Yu, H.C. Wu, S.Q. Xie, Bioorg. Med. Chem. Lett. 23 (2013) 2288–2292.
- [23] M.X. Li, Y.L. Lu, M. Yang, Y.K. Li, L.Z. Zhang, S.Q. Xie, Dalton Trans. 41 (2012) 12882–12887.
- [24] M.X. Li, D. Zhang, L.Z. Zhang, J.Y. Niu, B.S. Ji, J. Organomet. Chem. 696 (2011) 852–858.
- [25] M.X. Li, C.L. Chen, D. Zhang, J.Y. Niu, B.S. Ji, Eur. J. Med. Chem. 45 (2010) 3169–3177.
- [26] M. Joseph, V. Suni, C.R. Nayar, M.R.P. Kurup, H.K. Fun, J. Mol. Struct. 705 (2004) 63–70.
- [27] G.M. Sheldrick, Acta Crystallogr. Sect. A 64 (2008) 112–122.
- [28] T.A. Reena, E.B. Seena, M.R. Prathapachandra Kurup, Polyhedron 27 (2008) 1825–1831.
- [29] D. Kovala-Demertzi, M.A. Demertzi, J.R. Miller, C. Papadopoulou, C. Dodorou, G. Filousis, J. Inorg. Biochem. 86 (2001) 555–563.
- [30] X.R. Yue, Y.N. Chen, G.C. Yang, S.M. Yue, Z.M. Su, Synth. Met. 200 (2015) 1–6.
- [31] S. Singh, N. Bharti, P.P. Mohapatra, Chem. Rev. 109 (2009) 1900–1947.